Aircraft Observation of a Landfalling Pacific Front Upstream of Vancouver Island

Cheng-Ku Yu[1] and Bradley F. Smull[2]

Ben Jong-Dao Jou[1]

[1]Department of Atmospheric Sciences, National Taiwan University, Taipei, Taiwan

[2]NOAA/NSSL, and Department of Atmospheric Sciences, University of Washington, USA

1. INTRODUCTION

In contrast to relevant dynamics of terrain influence in the presence of steady, horizontally uniform onshore flow, which have been explored to some degree by previous studies, interactions of unsteady, diabatic flow (such as that associated with fronts and cyclones) with topography remain largely unexplored. Particularly, under suitably environmental conditions such interaction can result in the development of local intense rainfall and high surface winds occurring in the vicinity of the mountains (Mass and Ferber 1990; Overland and Bond 1993; Li and Chen 1998; Yu and Smull 2000). Unfortunately, the lack of detailed observations nearby topography has largely limited our knowledge of the severe weather conditions and underlying dynamical processes accompanying the orographic modification of these events, which in turn lead to a poor forecasting skill for their occurrence. Recent atmospheric field experiments [such as COAST (Bond et al. 1997) and Wet MAP (Houze et al. 1998)], which were conducted in the vicinity of the mountainous regions, have attempted to better document the mesoscale structure of orographically modified winds and precipitation and to investigate dynamical processes resulting in these alterations. The primary objective of this study is to use airborne Doppler radar and flight-level in situ data to investigate the mesoscale structure and evolution of a Pacific front as it made landfall on the coast of Vancouver Island on 13 December 1993 during the Coastal Observation And Simulation with Topography (COAST) experiment. We will show various aspects of the terrain influence on the modification of the front in terms of its kinematic, thermodynamic, and precipitation.

2. MESOSCALE ENVIRONMENT

Intensive observations by the NOAA P-3 were conducted in the coastal zone south of Vancouver Island between 0200 UTC and 0800 UTC on 13 December 1993 as a synoptic front seen from the National Meteorological Center (NMC) surface analysis was located over the western Pacific Ocean of the United States, extending from the north end of Vancouver Island to ~140° W between 50° N and 35° N. The plot of selected flight-level winds and sea-level pressure analysis provide important mesoscale aspects of low-level airflow in the vicinity of the front as shown in Fig. 1. The front was characterized by a sharp change in wind speed and slight windshift (a more obvious windshift observed near the coast) from strong southerly/south-southeasterly flow within the warm air mass to weak southerly/southwesterly flow within the cold air mass. The front was oriented approximately south-southwest—north-northeast so as to intersect the long axis of Vancouver Island at a significant angle. To the east of the front, there was an obvious wind transition from strong southerly flow (with a maximum of ~28 m s^{-1}) offshore to southeasterly flow near the coast. Winds near the coast were approximately parallel to the coast and highly ageostrophic, in contrast to more geostrophic southerlies farther offshore. The southerlies and associated pressure gradient were much weaker to the west of the front. Contours of potential temperature shown in Fig. 2 indicate that the air temperature within the nearshore blocked flow was colder than that offshore. The coldest air was found along the coast of southern Vancouver Island and was advected by the blocked southeasterly flow into the frontal zone. The nearshore cross-front temperature gradient was much weaker than that offshore. Less baroclinity near the coast is likely due to the influence of the nearshore colder blocked flow.

Thermodynamic profiles (Fig. 3) located ~30 km east of the front (~90 km offshore) indicate saturated situations below 3000 m (MSL) and convectively stable-to-neutral conditions through the layer. Stronger stratification was confined to the lowest 1000 m except a shallow, neutral layer near the surface. Winds veered with height from south-southeasterly flow near the surface to southwesterly flow at 850 mb, and exhibited a maximum of ~35 ms^{-1} at a

Corresponding author address: Dr. Cheng-Ku Yu, Department of Atmospheric Sciences, National Taiwan University, 61, Ln 144, Sec 4 Keelung Rd, Taipei, Taiwan. E-mail: yuku@hp735.as.ntu.edu.tw

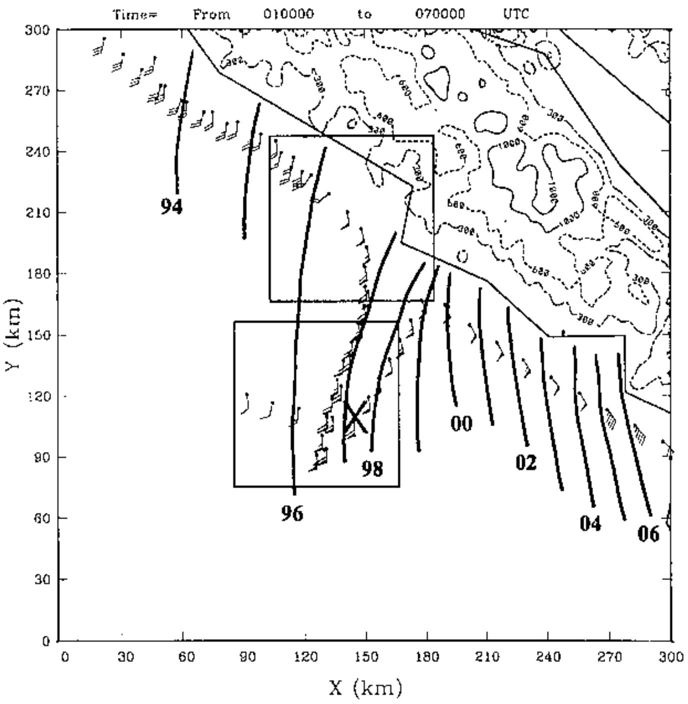

Fig. 1. Selected flight-level winds (wind flags and full wind barbs correspond to 25 and 5 m s^{-1}, half-barbs to 2.5 m s^{-1}) at and below ~350 m between 0100 and 0700 UTC and sea-level pressure (thick-solid lines) for the case of 13 December 1993. Terrain heights of 300, 600, and 1000 m are indicated by dashed-dotted, dashed, and solid contours, respectively. Inset two boxes locate 81 × 81 km^2 dual-Doppler analysis domains. The symbol "X" denotes the location of P-3 ascent sounding shown in Fig. 3.

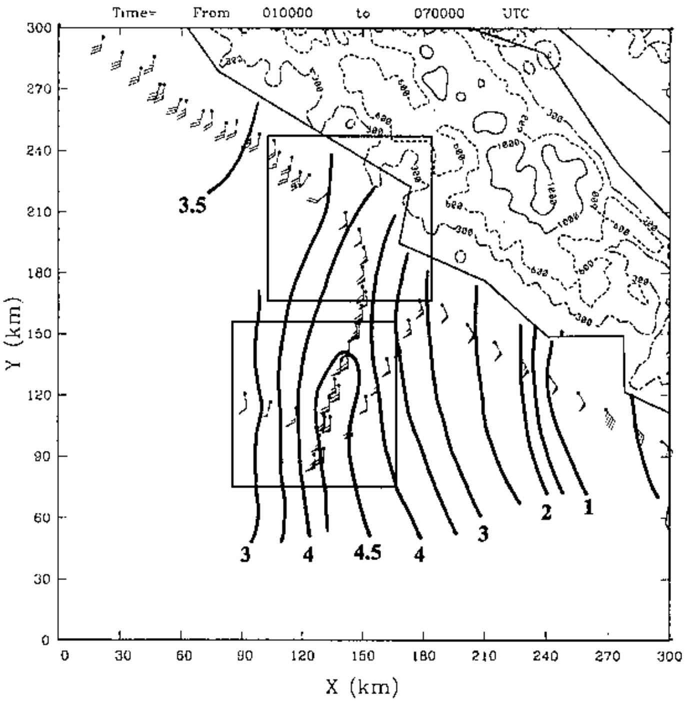

Fig. 2. As in Fig. 1 except showing contours of potential temperature with interval of 0.5 K.

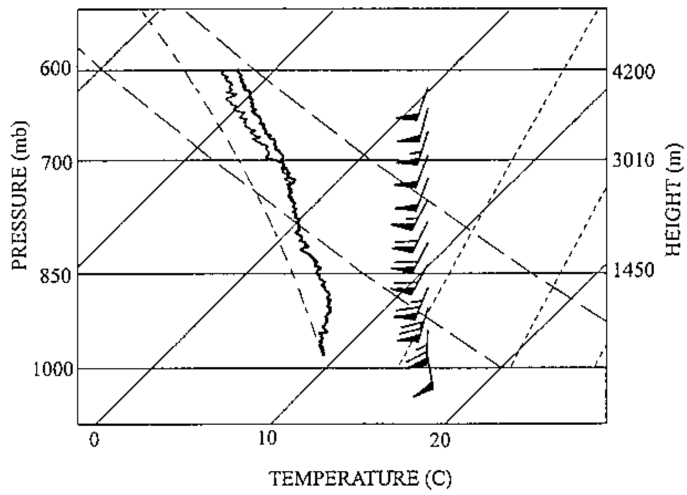

Fig. 3. Skew *T*-log*p* plot of P-3 ascent sounding (location refers to Fig. 1) from 200 to 4000 meters during the interval of 0205-0218 UTC. Corresponding winds are also indicated (wind flags and full wind barbs correspond to 25 and 5 m s^{-1}, half-barbs to 2.5 m s^{-1}).

height of ~1 km. For the case studied here, the terrain height (*H*) of Vancouver Island in the region of aircraft observation is ~1000 m (cf. Fig. 1), and the latitude of 50° gives a value of f= 1.1 × 10^{-4} s^{-1}. Since the air at low levels was saturated as shown in Fig. 3, static stability is approximated using the saturated Brunt-Väisälä frequency (N_m) derived by Durran and Klemp (1982) and is equal to 8.2 × 10^{-3} s^{-1}. The mountain half-width (*L*) is assumed to be ~50 km and the cross-barrier flow averaged below 1000 m (MSL) is equal to 23 ms^{-1}. With these values, we obtain the Froude number (Fr=*U/NmH*), Burger number (B=*HNm/fL*), and the Rossby radius of deformation (L_R=*NH/f*) equal to 2.8, 1.5, and 74 km, respectively, for the present case.

3. DUAL-DOPPLER OBSERVATIONS

Because the airborne Doppler observations were collected not only near the coast but also in a location ~150 km from the coastal barrier, they provide a detailed description of three-dimensional kinematic and precipitation fields in both nearshore and offshore regions. The locations of two dual-Doppler analysis domains are shown in Fig. 1. For convenience, the northern (southern) analysis domain is referred to as the nearshore (offshore) domain in the following discussions. Figure 4 shows winds and precipitation at the height of 0.5 km (all heights MSL) at 0635 UTC for the nearshore domain. The frontal zone was characterized by an obvious change in winds and was associated with an organized, heavier radar reflectivities (a maximum of ~25-30 dBZ). As evident in Fig. 1, a profound wind transition was observed within the

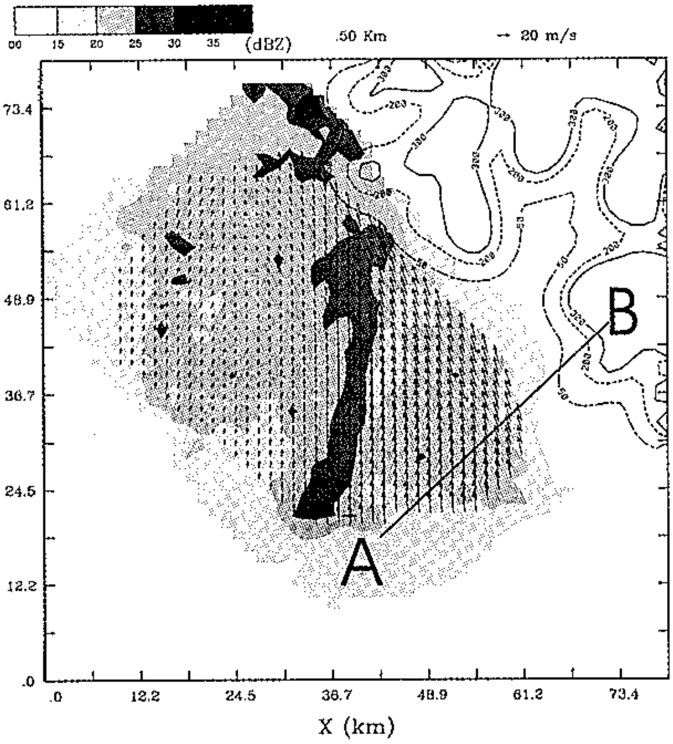

Fig. 4. Ground-relative wind vectors (key at upper right) and radar reflectivity (dBZ, key to shading at upper left) within the nearshore domain at 0.5 km MSL derived from the airborne dual-Doppler analysis at 0635 UTC. Terrain height thresholds of 50, 200, 300 m MSL are indicated by dashed-dotted, dashed and solid contours, respectively. Thick line segment A-B marks location of vertical cross section shown in Fig. 6.

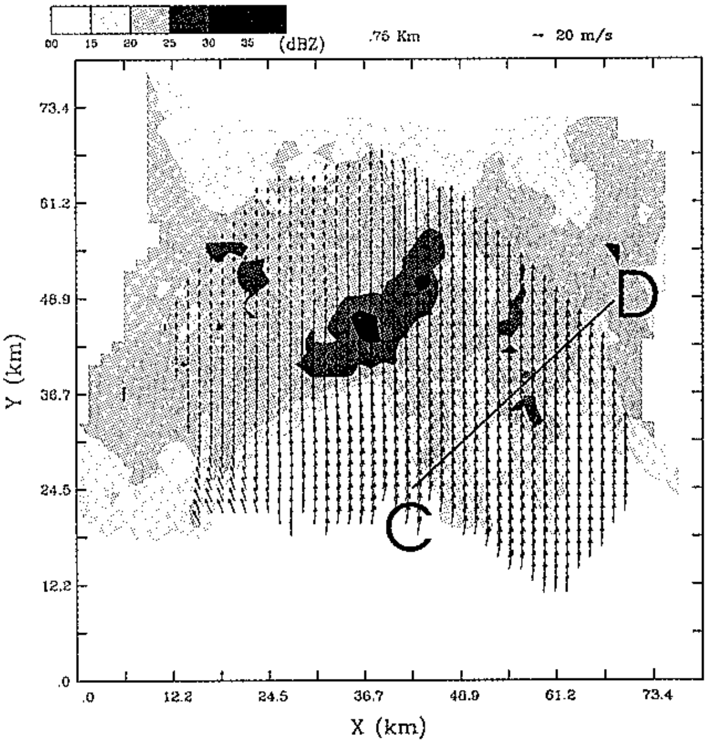

Fig. 5. As in Fig. 4 except showing the offshore domain at 0.75 km MSL at 0503 UTC. Thick line segment C-D marks location of vertical cross section shown in Fig. 7.

warm air mass from southerly flow offshore to south-southeasterlies near the coast. Winds within the cold air mass were southerlies and/or southwesterlies with much weaker magnitude, and appeared to be less influenced by the topography. Prior to 0635 UTC, a sequence of dual-Doppler synthesis results (not shown) indicates that the nearshore segment of the front remained stationary and its associated precipitation increased slightly during this period. The absence of frontal movement probably relates to the retardation by the nearshore blocked flow (e.g., Doyle 1997).

In contrast to an approximately south-north alignment near the coast, the front was oriented more southwest-northeast farther offshore as revealed by the results from the offshore domain (Fig. 5). Within the warm air mass, the flow was southerlies and no evidence of the rapid shift to south-southeasterly winds seen in the nearshore domain was observed. Two vertical sections of cross- and along-barrier velocities (AB indicated in Fig. 4 and CD indicated in Fig. 5) are selected to be perpendicular to the orientation of Vancouver Island [~43° from the north (counterclockwise)]. They clearly show that within the nearshore domain cross-barrier flow below 1 km decreased from ~22 ms^{-1} at a position 20 km offshore to ~16 ms^{-1} at the coast, with a concomitant increase in along-barrier flow (Fig. 6). This feature is in contrast to that observed within the offshore domain showing quite horizontally uniform cross- and along-barrier velocities at low levels (Fig. 7). Above the height of the coastal mountains (~1 km MSL), both of the vertical sections indicate a relatively unperturbed wind pattern. These results suggest that the orographically blocked zone only extended to a region ~68 km from the mountain crest of Vancouver Island (i.e., ~18 km from the coastline). This observed offshore extent is pretty close to the horizontal scale of the upstream influence of topography (i.e., the Rossby radius of deformation calculated in section 3) as predicted by idealized theory (Pierrehumbert 1984; Pierrehumbert and Wyman 1985).

The movement of the front observed farther offshore appeared to vary with time. As seen from the dual-Doppler analyses at different time periods, the southwest-northeast oriented front (cf. Fig. 5) initially progressed slowly northwestward (i.e., toward the cold air mass) with a speed of ~6 m s^{-1}. However, during the later part of observation (roughly after 0650 UTC) it became more south-north oriented and moved eastward more rapidly. The difference in frontal movement between the nearshore and offshore regions resulted in the occurrence of a pronounced inflection in the frontal windshift with its apex located ~25 km offshore as shown by the dual-Doppler synthesis within the nearshore domain at 0722 UTC (Fig. 8). The heavy dashed line in Fig. 8 locates the axis of maximum cyclonic vorticity, marking the frontal wi-

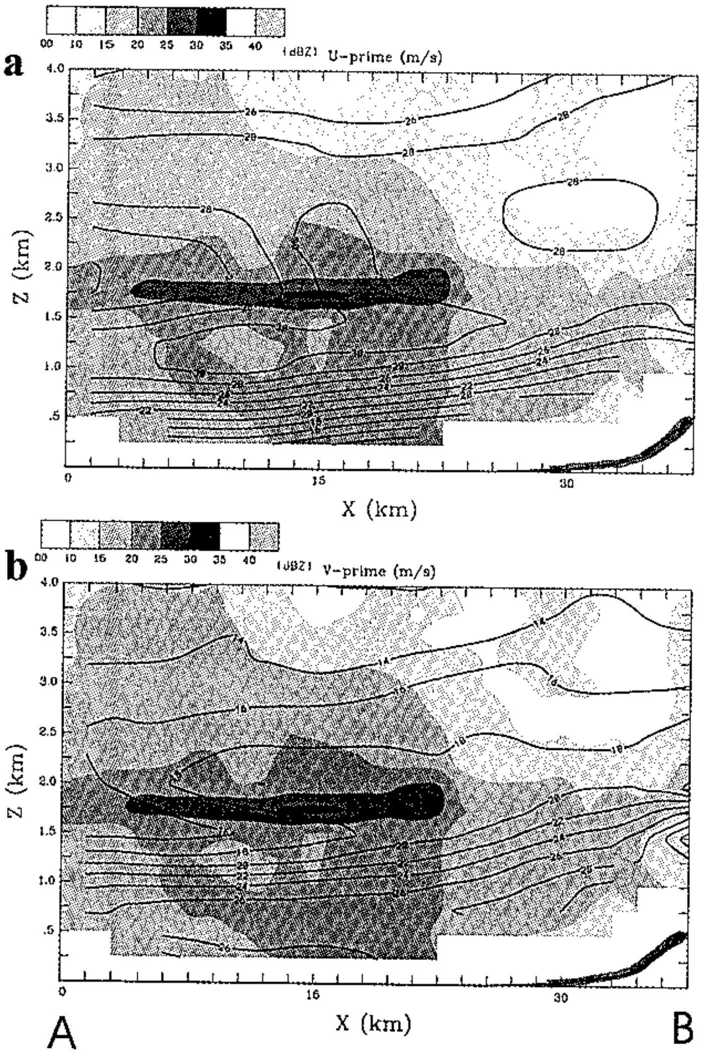

Fig. 6. Vertical cross section along A-B in Fig. 4 showing radar reflectivity (dBZ, shading key at upper left) in conjunction with (a) cross-barrier and (b) along-barrier component flow (2 m s^{-1} contour interval) at 0635 UTC. Heavy solid line in lower-right portion of each panel indicates height of coastal topography along the section.

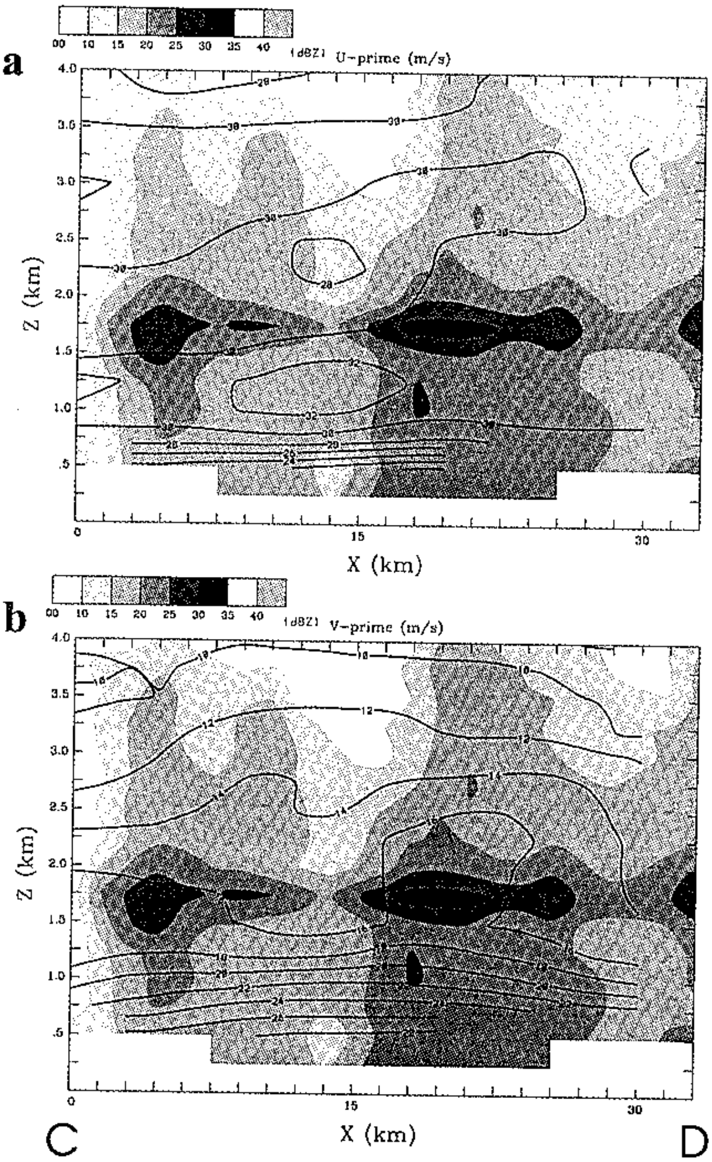

Fig. 7. As in Fig. 6 except along C-D in Fig. 5.

-ndshift zone. To the north of the inflection point, there was a locally enhanced convergence with maximum of ~2.8×10^{-3} s^{-1} (Fig. 8b), which is much greater than that of strongest convergence (~1.6×10^{-3} s^{-1}) observed along the front before the occurrence of the frontal inflection. In contrast, a near-zero, weak divergence (+ ~0-4×10^{-4} s^{-1}) was found near and to the south of the inflection point, which might contribute, at least partly, to the presence of weak radar echo (<15 dBZ) near the inflection point. Such dipole structure of the divergence field may relate to changes in the along- and cross-front flow components attributed to the difference of the frontal orientation on both sides of the inflection point.

4. CONCLUSIONS

This study uses airborne Doppler radar and flight-level observations to examine the mesoscale structure and evolution of airflow and precipitation in the vicinity of a Pacific front as it made landfall on the coast of Vancouver Island on 13 December 1993 during COAST. The Vancouver Island is approximately two-dimensional and oriented roughly northwest-southeast, with an elevation of ~1000 m MSL and a mountain width of ~50 km. Our results show that airflow within the warm air mass was blocked by the topography, with a profound wind transition from southerly flow offshore to south-southeasterlies near the coast. The orographically blocked zone was found to extend only to a region ~18 km offshore and confined to the lowest 1000 m MSL. Modulations of the frontal intens-

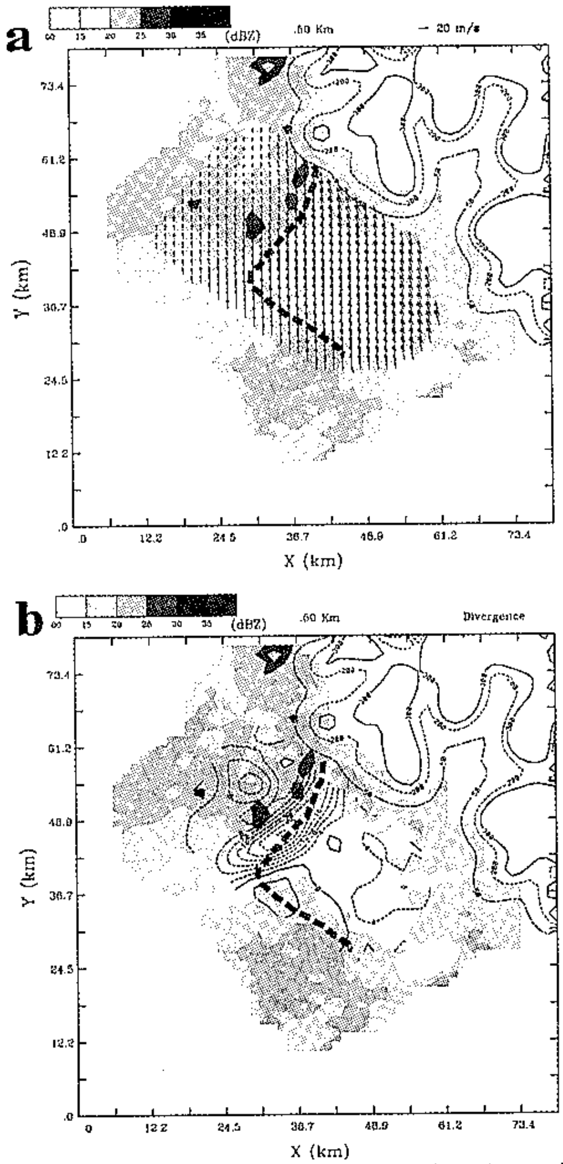

Fig. 8. Ground-relative wind vectors (a) with key at upper left, and horizontal divergence (b) with contour interval 4×10^{-4} s^{-1} within the nearshore domain at 0.5 km MSL derived from the airborne dual-Doppler analysis at 0722 UTC. The frontal windshift zone is marked by the heavy dashed line. Terrain height thresholds of 50, 200, 300 m MSL are indicated by dashed-dotted, dashed and solid contours, respectively.

-ity and movement by the coastal terrain were also evident. The nearshore segment of the front exhibited less baroclinity and appeared to be stationary and strongly retarded. In contrast, the offshore segment of the front generally moved at a considerable speed. Particularly, the difference in frontal moving speeds between nearshore and offshore resulted in an obvious inflection in the frontal windshift zone. Our analysis suggests that divergence perturbations generated by processes associated with the occurrence of the frontal inflection may have led to modifications of precipitation along the front. While locally enhanced and/or reduced precipitation intensity near the inflection point as the front goes under the influence of the orography have been observed in other frontal cases such as that observed along the west coast of the United States (Braun et al. 1997) and Taiwan area (Trier et al. 1990), their associated processes have been poorly understood due to the lack of detailed and continued observation over a region where the inflection point occurs.

References

Bond, N. A., C. F. Mass, B. F. Smull, R. A. Houze, Jr., M.-J Yang, B. A. Colle, S. A. Braun, M. A. Shapiro, B. R. Colman, P. J. Neiman, J. E. Overland, W. D. Neff, and J. D. Doyle, 1997: The Coastal Observations and Simulations with Topography (COAST) experiment. *Bull. Amer. Meteor. Soc.*, **78**, 1941-1955.

Braun, S. A., R. A. Houze, Jr. and B. F. Smull, 1997: Airborne dual-Doppler observations of an intense frontal system approaching the Pacific Northwest coast. *Mon. Wea. Rev.*, **125**, 3131-3156.

Doyle, J. D., 1997: The influence of mesoscale orography on a coastal jet and rainband. *Mon. Wea. Rev.*, **125**, 1465-1488.

Durran, D. R., and J. B. Klemp, 1982: On the effects of moisture on the Brunt-Väisälä frequency. *J. Atmos. Sci.*, **39**, 2152-2158.

Houze, R.A., Jr., J. Kuettner, and R. Smith, Eds., 1998: Mesoscale Alpine Programme U.S. Overview Document and Experiment Design. UCAR, Boulder, Colorado, 30 pp. (available from UCAR via email request to rjm@ucar.edu).

Li, J., and Y.-L. Chen, 1998: Barrier jets during TAMEX. *Mon. Wea. Rev.*, **126**, 959-971.

Mass, C. F., and G. K. Ferber, 1990: Surface pressure perturbations produced by an isolated mesoscale topographic barrier. Part I: General characteristics and dynamics. *Mon. Wea. Rev.*, **118**, 2579-2596.

Overland, J. E., and N. A. Bond, 1993: The influence of coastal orography: The Yakutat storm. *Mon. Wea. Rev.*, **121**, 1388-1397.

Pierrehumbert, R. T., 1984: Linear results on the barrier effects of mesoscale mountains. *J. Atmos. Sci.*, **41**, 1356-1367.

Pierrehumbert, R. T., and B. Wyman, 1985: Upstream effects of mesoscale mountains. *J. Atmos. Sci.*, **42**, 977-1003.

Trier, S. B., D. B. Parsons, and T. J. Matejka, 1990: Observations of a subtropical cold front in a region of complex terrain. *Mon. Wea. Rev.*, **118**, 2449-2470.

Yu, C.- K., and B. F. Smull, 2000: Airborne Doppler observations of a landfalling cold front upstream of steep coastal orography. *Mon. Wea. Rev.*, **128**, 1577-1603.